

Coke Size Degradation and Its Reactivity Across the Tuyere Regions in a Large-Scale Blast Furnace of Hyundai Steel



TAE JUN PARK, KWANG HYUN KO, JONG HYUP LEE, SUSHIL GUPTA, VEENA SAHAJWALLA, and BYONG CHUL KIM

It has been well recognized that coke samples can be effectively taken out of working blast furnaces using a drilling machine at the tuyere level. The core represents samples with different temperature profiles at various tuyere regions of a large blast furnace. The average coke size at the tuyere level is known to be about 50 pct smaller than the charged cokes. Using fixed bed reactor and XRD techniques, the cokes sampled were studied for CO₂ reactivity and crystallinity, respectively. The apparent reaction rate of coke rapidly increases in the raceway zone, followed by a decrease as the samples are taken at deeper sites in the furnace where the Fe₂O₃ and CaO contents are high in the bosh and raceway zones in the high temperature regions. In this study, samples extracted at the tuyere level of a large blast furnace were examined to characterize the coke size degradation and the effect of coke graphitization on the reactivity and fines generation at various locations around the tuyere level.

<https://doi.org/10.1007/s11663-020-01806-y>

© The Minerals, Metals & Materials Society and ASM International 2020

I. INTRODUCTION

THE blast furnace (BF) is expected to maintain its dominant status in the ironmaking process using iron ore in the future.^[1,2] Increasing environmental concerns associated with making coke are influencing the economy of the BF route for steelmaking. To maintain the competitiveness of the blast furnace, the steel industry is looking for opportunities to reduce the reliance on coke consumption in BFs.^[3]

To reduce the coke consumption rate and increase productivity, supplementary fuels, such as pulverized coal, oil, and gas, are injected through the bottom of the blast furnace. The pulverized coal is considered the most popular supplementary fuel. There have been extensive studies with various aspects of injected fuels, mainly limited to improving the combustion of coal.^[4-6] Coke reacts with CO₂ during its descent deep inside of the blast furnace and produces CO to be used as the

reducing agent for the reduction of iron ore in the upper part of the blast furnace.^[7] This means that high CSR along with low CRI is a prerequisite for coke to withstand the extreme conditions in the blast furnace. This is because the high reaction rate of coke with the oxidizing agent in the blast furnace causes coke to be rapidly weakened and catastrophically degraded into smaller particles, consequently leading to poor permeability, decreasing efficiency of blast furnace performance, and low permeability at the edge of the raceway by coke residue.

The current coke quality parameters are measured in simple tests at relatively low temperatures and at atmospheric pressure and as such are constrained by their inability to simulate some of the phenomena of a working BF at extremely high pressure and temperature, such as the graphitization and coke reactions that occur in the very active zone adjacent to the tuyere level. Due to the complexity of reactions in the blast furnace with high temperatures and pressures, it was hard to extract representative coke samples from working furnaces. Recently, however, a tuyere core-drilling technique has enabled operators to effectively extract coke samples from an operating blast furnace, thereby providing a source of potentially useful information about various important phenomena at working conditions.^[8-14]

In recent years, the number of steel companies operating large-scale blast furnaces has grown to increase production of molten iron. Therefore, there is a need to characterize the behavior of coke fines

TAE JUN PARK, KWANG HYUN KO, JONG HYUP LEE, and BYONG CHUL KIM are with the Ironmaking Research Team, R&D Center, Hyundai-Steel Company, 1480 Bukbusaneop-ro, Dangjin-Si, Chungnam, 31719, Republic of Korea. Contact e-mail: bckim@hyundai-steel.com SUSHIL GUPTA and VEENA SAHAJWALLA are with the School of Materials Science and Engineering, The University of New South Wales, Sydney, NSW 2052, Australia.

Manuscript submitted November 9, 2019.

Article published online March 9, 2020.

generation in different regions of a large BF to understand the degradation behavior of coke in the large-scale blast furnace.

In this article, core samples extracted from a large blast furnace at the tuyere level have been examined to characterize coke size degradation and graphitization behavior at various locations. The effects of coke graphitization on the modification of reactivity and fines generation are also discussed.

II. MATERIALS AND METHODS

A. Tuyere Drilling and Sample Selection

In this study, tuyere-level coke samples were obtained from a blast furnace of Hyundai Steel Company at Dangjin, South Korea. The blast furnace configuration is summarized in Table I. Specially designed mobile tuyere drilling equipment was used to extract the coke samples from one of the tuyeres (Figure 1). A steel core drill was placed into the working blast furnace to the center of the furnace through an open tuyere to extract coke from differently heat treated regions and then cooled down after withdrawing. Figure 2 shows the steel core drill with cokes withdrawn from the furnace introducing a wide range of coke particles. Collected samples were categorized into 12 domains at regular intervals (25 cm).

A large fraction of iron and slag particles was present within the coke particles. To reduce experimental error, screening of the iron and slag fractions was carried out first, and then clean pieces of cokes were collected for a series of experiments. Particle size between 19 to 26.5 mm was selected as a representative sample size for the L_C value and reactivity.

B. Characterization of the Carbon Structure by XRD

The PANalytical Xpert multipurpose X-ray diffraction system (MPD) at the University of New South Wales was used for carbon structure analysis. XRD can provide the typical graphite parameters of the crystallites in the carbonaceous materials, *i.e.*, the interlayer spacing between graphene planes (d_{002}), and average height of the crystallites (L_C); 35 Kv and 30 mA copper K radiation was used to scan over the angular 2θ range of 5–90 deg. Microcrystalline sizes of coke samples heat treated at different temperatures were calculated using the Bragg and Scherer equation shown below:

$$L_C = 0.89\lambda / (B \cos \theta)$$

where λ is the X-ray wavelength (1.544 Å), B is the angular (2θ) width of the corresponding peak at the half maximum intensity, and θ is the peak position. With this background and existing theoretical model,^[15] the calculation of the L_C value with the software was proved in a previous study.^[14]

C. Coke Reactivity

Coke samples were dried at 373 K for 4 days to make sure to remove the unwanted moisture content; 0.5 g of sample was taken for the reactivity test in the fixed bed reactor (FBR). All reactivity tests were carried out at 1198 K, which was the temperature of the samples measured by the thermocouple. Figure 3 shows a schematic of the fixed bed reactor system. The reactor system consisted of a fixed bed of sample supported in a quartz reaction tube by a sintered glass frit. The quartz tube was placed in an electrically heated furnace. Before loading the quartz tube into the furnace, the quartz tube was purged by nitrogen at a flow rate of 1 l/min for 60 min to make sure the unwanted residual air in the tube was properly removed. The design of the reactor allowed a thermocouple to measure the temperature in the center of the sample bed. Once the reaction temperature became stable at around 1198 K, the reactant gas (CO₂, 99.999 pct) was passed through the sample bed from top to bottom at a flow rate of 0.75 l/min. A mass-flow controller controlled the flow rate of the gas. Before entering the reactor, the reactant gas and purging gas (N₂, 99.999 pct) were passed through an oxygen trap and a Drierite column to remove traces of oxygen and moisture, respectively. After the reaction, the sample was naturally taken outside of the furnace by nitrogen at a flow rate of 1 l.

The concentration of CO in the exhaust gas was measured continuously using an infrared analyzer (IR), and the change in the CO concentration was automatically transferred to a computer system.

D. Proximate Analysis of Coke

The moisture content of the sample was measured at 383 K for 10 min, and then the temperature was heated up to 1223 K. The temperature was held at 1223 K in inert gas condition to weigh the mass of fixed carbon. Then, the atmosphere was switched to air for 60 min to consume all the carbon content. Then, the weight of ash was obtained.

III. RESULTS AND DISCUSSION

A. Coke Size Distribution Across Tuyere Regions

Figure 4 shows a change in the coke size, on average, in each section at the tuyere level. The actual core insertion length was about 5.2 m, and the sampling length was about 2.9 m, which is attributed to 55.8 pct compression of samples during the drilling. The core represents samples with a different temperature profile at various tuyere regions of the blast furnace. The bosh is adjacent to the tuyere. The raceway has the highest temperature zone of a blast furnace. The “bird’s nest” region is usually associated with accumulation of hot metal, while the “deadman” region is featured as an

Table I. Blast Furnace Operation, Production and Coke Quality Data

Operation Data		Production Data		Coke Data	
Inner Volume (m ³)	5,250	hot metal (t/d)	12,000	DI (pct)	88.7
Hearth Diameter (m)	14.8	reducing agent (kg/thm)	500	CSR (pct)	64.4
Number of Tuyeres (EA)	42	coke rate (kg/thm)	337	MS (pct)	51.3
Oxygen Enrichment (Nm ³ /h)	26,874	PCR (kg/thm)	163	Ash (pct)	11.6



Fig. 1—Schematic diagram of the drilling equipment used to extract the coke samples at the tuyere.

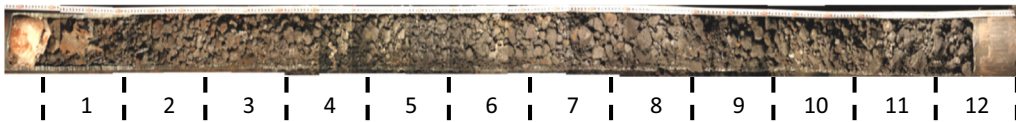


Fig. 2—Schematic 12 domains of the steel probe.

accumulation of the finest material, which tends to stop gas from flowing up.^[3] The average coke size at the tuyere level was 50 pct smaller than the charged cokes, which was initially 51.3 mm. In the past, tuyere sampling and blast furnace dissection studies reported that the feed coke size decreased by at least 50 pct as it descended to the tuyere level.^[3] According to our result, the at least 50 pct size reduction of coke in the tuyere region is in full agreement with previous studies.

The average particle size in the raceway zone was the smallest among the samples, but subsequently increased at the bird's nest and deadman zones. This phenomenon was attributed to the high blowing pressure with a large amount of oxygen blown through the tuyere, resulting in rapid coke consumption, accompanied by a catastrophic abrasion and burning of coke in the bosh and raceway zones. The length of each zone was calculated to reflect the compression ratio shown above. Accordingly, each reaction region can be assigned to a different position in

Figure 2. The bosh region in this core is located over 0.9–1.1 m (about 0.2 m), the raceway region covers from 1.1 to 2.8 m (about 1.7 m), the bird's nest region takes place from 2.8 to 4.1 m (about 1.3 m), and beyond 4.1 m (about 1.1 m) it is considered the deadman zone.

Figure 5 shows the variation of the fraction for fine particles < 2.8 mm as a function of the distance from the tuyere. The fraction of particles < 2.8 mm (– 2.8 mm) in the tuyere region can be used as an indicator of three phenomena, *i.e.*, the state of bed permeability, the raceway depth, and the coke CSR.^[17] The highest fraction of the – 2.8 mm fine incidence rate was observed in the bird's nest and deadman zones.

The actual fraction of coke fines in the tuyere regions could also be influenced by gasification and prolonged carburization reactions particularly in the deadman section and also could be attributed to local gas flows in the raceway.

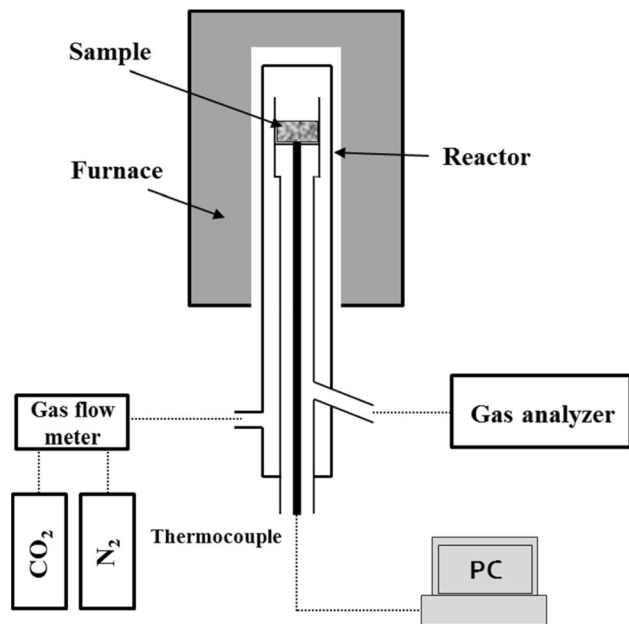


Fig. 3—Schematic diagram of the fixed bed reactor system used for CO₂ gasification.

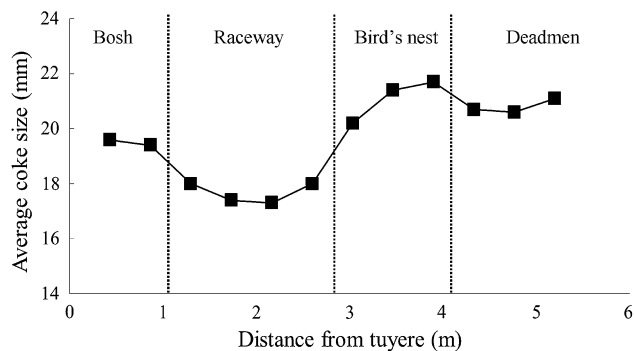


Fig. 4—Average coke size and classification of zones according to the tuyere distance.

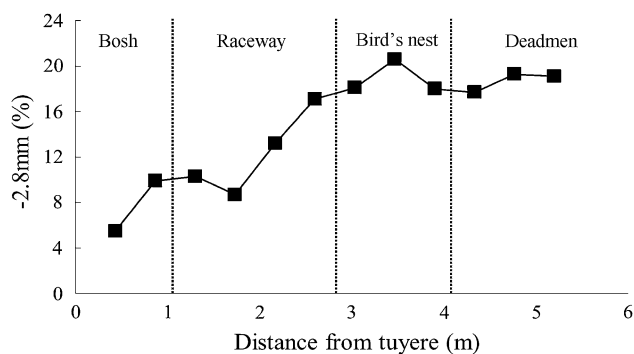


Fig. 5—The -2.8 mm fine percentage according to the tuyere distance.

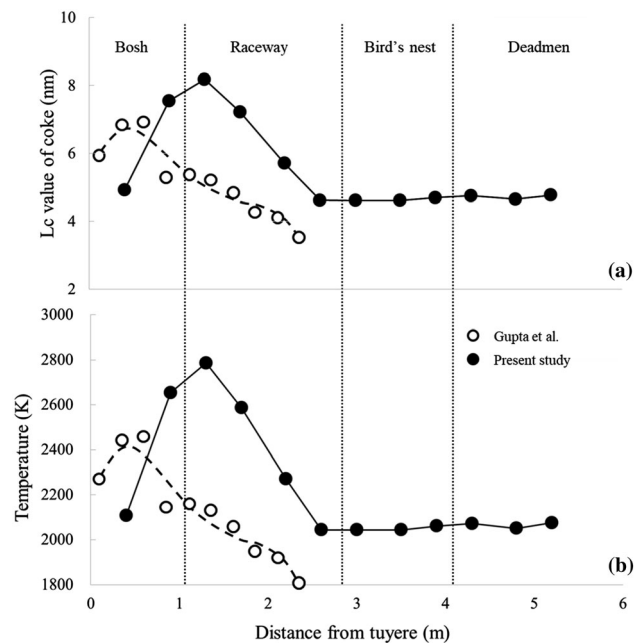


Fig. 6—Change of the L_c value (a) and the estimated temperature (b) with distance from the tuyere (× feed coke L_c value: 1.2295, estimated temperature: 1338 K).

B. Carbon Structure of Cokes Across Tuyere Regions

Figure 6 shows that the L_c value and the calculated temperature of cokes decreased with the distance away from tuyere entrance. It is not possible to directly measure the tuyere region temperatures. However, the calculated temperatures of cokes in the tuyere regions derived by the L_c value were fully in agreement with previous studies based on direct measurements and previous dissection studies.^[14,15] The L_c value was high at the bosh and raceway, but others showed a similar value in the bird's nest and deadman zones. Based on these results, the temperature of the blast furnace was calculated to be > 2000 K for most coke, and the highest temperature was calculated as 2800 K adjacent to the raceway. After that, the temperature decreased as a function of the distance away from the tuyere, and the temperatures of the bird's nest and deadman zones were similar.

The temperature profile of the large blast furnace (> 5500 Nm³) at the tuyere level is high compared with the previous^[16] small blast furnace. This is a distinct feature of the large-scale blast furnace because of the relatively large blowing rate and the amounts of oxygen that are blown at the same time, and large amounts of coke and pulverized coal are charged. The actual temperatures in the deadman zone may be slightly lower than the calculated temperatures because the additional heat treatment by molten iron provides coke with more opportunity to align the basic structural units in a more highly ordered form like graphitizing carbon.^[3]

As shown in Figure 6, the patterns of heat treatment temperatures of cokes corresponding to a variation of L_c values are identical to those in a previous study carried out with coke from a smaller size furnace.^[16]

C. Reactivity of Cokes Under CO_2 Atmosphere

Figure 7 shows the apparent reaction rate of cokes as a function of distance from the tuyere entrance. The apparent reaction rate of coke rapidly increases in the raceway zone, which was followed by decreasing with distance away from the tuyere. It is believed that an increase in heat treatment results in the formation of a denser and more ordered carbon structure by lowering the number of activation sites available for the chemical activation process.^[17]

Therefore, coke undergoing increasing temperatures during the descent to the bottom of the blast furnace should prevent the oxidizing gases from penetrating into the core of coke because of the increased hardness, with the well-ordered carbon structure of coke having less active sites.

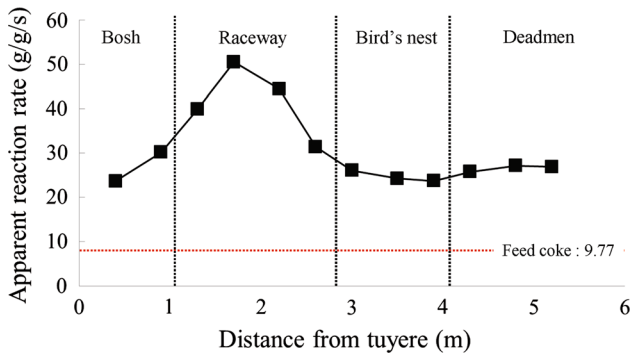


Fig. 7—Variation of the apparent reaction rate at 10 wt pct of carbon conversion with distance from the tuyere.

However, the results of reactivity are counterintuitive with an L_c pattern varying with temperature. As shown in Figure 6, coke at the raceway was exposed to the highest temperature in the furnace, thus resulting in formation of the more densely ordered carbon structure. There must be other factors at work, leading to an increase in the reactivity other than temperature.

The presence of ash contents in carbon materials also has a significant influence on altering the reactivity behavior during the gasification process. The majority of inorganic elements of coke as oxide are silica (SiO_2), alumina (Al_2O_3), iron oxide (Fe_2O_3), and calcium oxide (CaO) with a small amount of alkalis, alkaline earth as well as sulfur (S) and phosphorus (P). The total amount and type of minerals are dependent on where the coke is located in the furnace. The total amount of iron, calcium, *etc.*, measured by oxide ash analysis is a good indicator of the catalytic reaction, and the amount of catalytic minerals of iron and calcium-bearing oxides is proportional to an increase in coke reactivity (Table II). To interpret a conflicting trend between the heat treatment and reactivity, a correlation of the types and amount of selective ashes (Fe_2O_3 , CaO , K_2O , and Na_2O) in the cokes with reactivity was studied.

Figure 8 shows a variation of wt pct of Fe_2O_3 and CaO in coke ash with distance from the tuyere. The contents of Fe_2O_3 and CaO are high in the bosh and raceway zones, which are relatively high temperature regions. Figure 9 shows microscopic images of typical tuyere cokes from each of the zones. Figures 9(a) and (b) clearly show the hot metal droplets sticking on the surface of cokes. But (c) and (d) are not show molten iron. It was difficult to completely remove the penetrated molten iron from cokes in all the samples leading to high iron levels (> 10 pct). The presence of molten iron contents varies with distance from the tuyere, and the maximum amount of iron content was observed in the raceway zone. According to previous studies,^[17,18] graphitization of coke can take place more favorably

Table II. Proximate and Oxide Analysis of Cokes

	FC	1	2	3	4	5	6	7	8	9	10	11	12
Proximate Analysis (Wt Pct)													
Moisture	0.5	0.3	0.3	0.2	0.3	0.2	0.3	0.2	0.2	0.3	0.1	0.1	0.1
Ash	11.6	14.7	13.9	9.3	19.6	19.6	11.4	12	11.9	11.5	12.4	11.4	11.7
Elements as Oxide (Wt Pct)													
SiO_2	51	31.6	25.2	22.9	28.3	28.2	28.1	34	35.8	36.3	34.7	33.7	33.2
Al_2O_3	30.3	25	40.6	24.7	23.4	21.6	31	28.5	28	29	28.1	31.2	29.9
TiO_2	1.47	1.3	1.45	1.81	0.98	0.93	1.6	1.5	1.4	1.44	1.42	1.53	1.45
Fe_2O_3	8.5	22.3	25.1	40.7	28	25.4	19.2	13.4	13.8	13.1	18.2	14.5	15.6
CaO	2.58	15.5	2.6	6.8	16.7	19.4	5.6	4.17	4.03	3.93	3.38	4	4.23
MgO	1.2	1.43	1.68	0.26	0.74	1.91	3.07	2.51	2.35	2.56	2.31	2.66	2.73
K_2O	1.29	0.93	1.29	0.08	0.1	0.18	5.5	8.6	8.8	8	7.8	7.1	7.3
Na_2O	1.18	0.08	0.09	0.1	0.02	0.05	1.38	2.38	2.18	1.82	1.47	1.08	1.33
SO_3	0.63	1.01	0.37	0.56	1.09	1.31	2.11	1.69	1.59	1.18	0.79	1.35	1.75
P_2O_5	1.06	0.36	0.25	0.2	0.24	0.32	0.69	0.71	0.73	0.74	0.66	0.75	0.74
Mn_3O_4	0.06	0.28	0.21	0	0.07	0.13	0.75	0.99	0.83	0.81	0.78	0.74	0.69

at well below the normal graphitization temperature with assistance from the catalytic effect of molten iron in the blast furnace. Therefore, the effect of Fe on increasing the reactivity and L_c value of coke in the bosh and raceway zones cannot be ignored in this study.

The occurrence of the oxygen transfer mechanism also leads to the dissociative chemisorption of oxygen on both the CaO catalyst and active sites of the char under CO_2 atmosphere. This reaction forms a higher surface oxide (either superoxide or peroxide) over CaO. This reaction facilitates faster oxygen transfer to the carbon matrix, thus enhancing a favorable Boudouard reaction. Coke samples from 1 to 5 contain a higher wt pct of CaO compared with the other cokes.

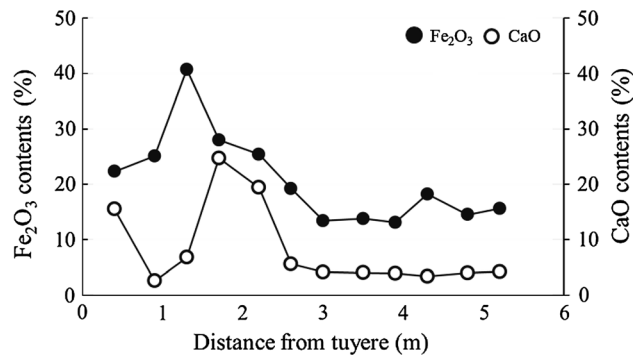


Fig. 8—Variation of wt pct of Fe_2O_3 and CaO in coke ash with distance from the tuyere.

On the other hand, the contents of K_2O and Na_2O are very small in the bosh and raceway zones (Figure 10). Higher contents of K_2O and Na_2O are observed from the bird's nest to deadman zone. The reduction of Na_2O and K_2O to their metallic elements becomes thermodynamically feasible at 923–973 K during the pyrolysis process. With increasing pyrolysis temperature up to 1373 K, the carbon reduction of the oxides to metals eventually becomes possible.^[19,20] Temperatures at the bosh and raceway (samples 1 to 5) are much higher than the reduction temperature for Na_2O and K_2O . Therefore, K and Na are almost devolatilized at the bosh and raceway zone, while others contain a large amount in oxide form because of low temperatures. The reduction to metallic K and Na in the carbon matrix is known to have a strong catalytic effect due to an intercalation reaction during gasification. However, as shown in Figure 11, Si mostly remained in the char in the form of SiO_2 at the bird's nest and deadman zones, thus deactivating alkali metals by forming inactive silicate (e.g., either K_2SiO_3 or KAlSiO_4). The formation of the silicate also leads to a lower reactivity.^[19] Therefore, no or less intercalation effect is expected from K and Na for the bird's nest and deadman zones (samples 6 to 12).

As described above, the increased reactivity is assigned to a combination effect of various types and amounts of ashes. Therefore, it is necessary to describe the overall influence of catalysts on the behavior of coke gasification. The CaO and Fe_2O_3 in the cokes act as a major driving force to affect the overall gasification rate.

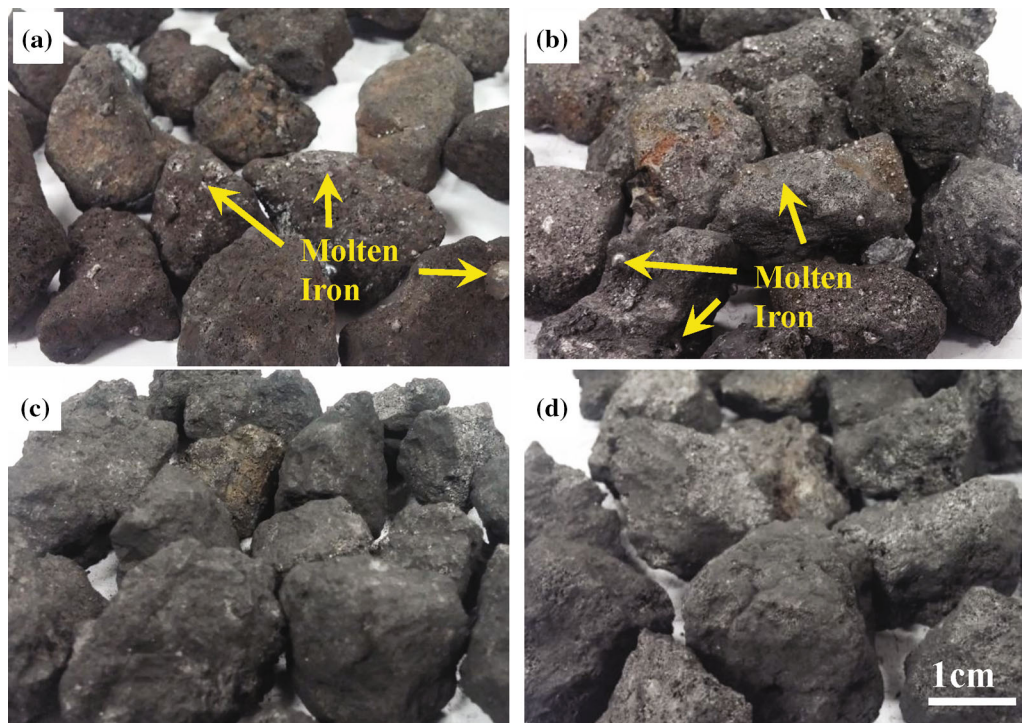


Fig. 9—Typical coke samples of different parts of the core. (a) Bosh; (b) raceway; (c) bird's nest; (d) deadman.

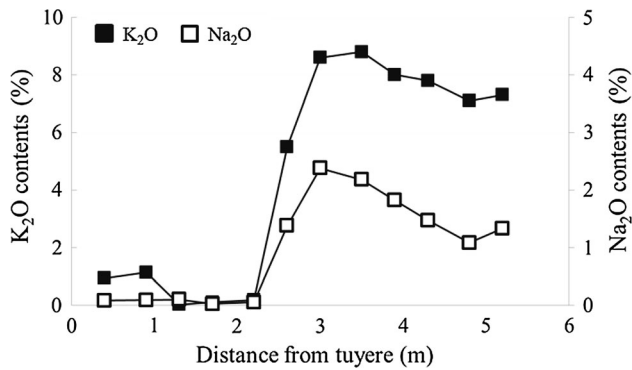


Fig. 10—Variation of weight percent of K₂O and Na₂O in coke ash with distance from the tuyere.

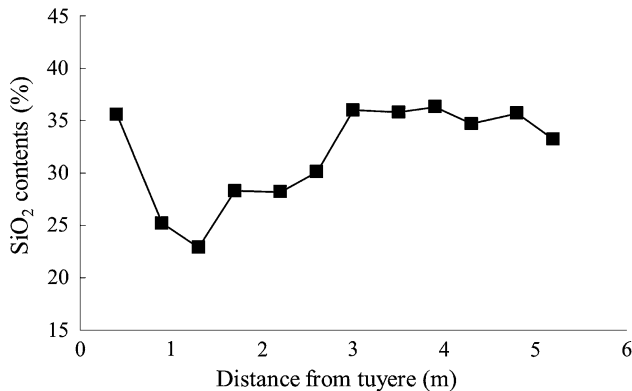


Fig. 11—Variation of weight percent of SiO₂ in coke ash with distance from the tuyere.

IV. CONCLUSION

The reactivity and carbon structure of coke sampled from a large-scale working blast furnace were studied with fixed bed reactor and XRD techniques, respectively. The variation of crystallite size and reactivity of coke were investigated. The following conclusions were drawn:

1. The crystallite size of carbon was strongly affected by the temperature in the furnace. The temperature of the blast furnace was calculated to be > 2000 K for most coke, and the highest temperature was calculated at 2800 K adjacent to the raceway.
2. A counterintuitive result of an increase in the reactivity of coke over the raceway zone was attributed to the presence of higher Fe and Ca bearing minerals. A higher content of alkali metals in coke over the bird's nest and deadman zone did not effectively increase the reactivity. The effect of Fe on increasing the

reactivity and L_c value of coke in the bosh and raceway zones cannot be ignored in this study

3. Si mostly remained in the char in the form of SiO₂ at the bird's nest and deadman zones, and the formation of the silicate also led to lower reactivity. Therefore, the CaO and Fe₂O₃ in the cokes act as a major driving force to affect the overall gasification rate.

REFERENCES

1. M.H. Best, J.A. Burgo, and H.S. Valia: *61st Ironmaking Conf. Proc.*, Nashville, TN, March 10–13, 2002, vol. 61, ISS Publication, Warrendale, PA, pp. 213–39.
2. J.P. Birat, F. Hanort, and G. Danloy: *Proc. 3rd Int. Conf. on Science and Technology of Ironmaking (ICSTI)*, Düsseldorf, Germany, 2003, pp. 588–92.
3. S. Gupta, V. Sahajwalla, J. Burgo, P. Chaubal, and T. Youmans: *Metall. Mater. Trans. B*, 2005, vol. 36B, pp. 385–94.
4. K. Ishii: *Advanced Pulverised Coal Injection Technology and Blast Furnace Operation*, 1st ed., Pergamon Press, Oxford, UK, 2000.
5. J.K. Chang and N.S. Hur: *ISIJ Int.*, 1997, vol. 2, pp. 119–25.
6. Y. Kazuyoshi, U. Hiromitsu, and T. Kenji: *ISIJ Int.*, 1992, vol. 6, pp. 716–24.
7. T. MacPhee, L. Giroux, K.W. Ng, T. Todoschuk, M. Conejeros, and C. Kolijn: *Fuel*, 2013, vol. 114, pp. 229–34.
8. R.R. Willmers: *Metall. Res. Technol.*, 1992, vol. 89, pp. 241–50.
9. O. Kerkkonen: *Iron and Steel Technology Conference Proceedings*, 2004, September 15–17, pp. 469–81.
10. R. Kanniala and O. Kerkkonen: *AISTech Proceedings*, Indianapolis, 2007, May 7–10, pp. 111–20.
11. S. Dong, N. Paterson, D. Dugwell, and R. Kandiyoti: *Energy Fuels*, 2007, vol. 21, pp. 3446–54.
12. S. Gupta, A. Wasaya, O. Kerkkonen, R. Kanniala, D. Osborne, and V. Sahajwalla: *AISTech Proceedings*, Pittsburgh, 2008, May 5–8, pp. 107–18.
13. K. Li, J. Zhang, M. Sun, C. Jiang, Z. Wang, J. Zhong, and Z. Liu: *Fuel*, 2018, vol. 225, pp. 299–310.
14. Z. Weljl, S. Ting, Z. Qifeng, C. Yinping, Q. Hui, W. Xinci, L. Jing, Z. Qun, Y. Guangzhi, and Y. Junhe: *Fuel*, 2019, vol. 251, pp. 218–23.
15. Z. Ye, S. Gupta, D. French, O. Kerkkonen, R. Kanniala, and V. Sahajwalla: *Energy Fuels*, 2013, vol. 27, pp. 4077–83.
16. S. Gupta, Y. ZhuoZhu, K. Riku, K. Olavi, and V. Sahajwalla: *Fuel*, 2013, vol. 113, pp. 77–85.
17. W. Wang, K.M. Thomas, R.M. Poultney, and R.R. Willmers: *Carbon*, 1995, vol. 33, pp. 1525–35.
18. B. Feng, S.K. Bhatia, and J.C. Barry: *Carbon*, 2002, vol. 40, pp. 481–96.
19. M.P. Kannan and G.N. Richards: *Fuel*, 1990, vol. 69, pp. 999–1006.
20. T.G. Devi and M.P. Kannan: *Energy Fuels*, 1999, vol. 14, pp. 127–30.

Publisher's Note Springer Nature remains neutral with regard to jurisdictional claims in published maps and institutional affiliations.